Coherent Light induced in Optical Fiber by a Charged Particle

X. Artru, C. Ray

Coherent Light induced in Optical Fiber by a Charged Particle

2016 J. Phys.: Conf. Ser. 732 012005

(http://iopscience.iop.org/1742-6596/732/1/012005)

Coherent Light induced in Optical Fiber by a Charged Particle

Xavier Artru[1,2] **and Cédric Ray**[1,3]

[1] Université de Lyon, Université Lyon 1, F-69622 Villeurbanne, France
[2] Institut de Physique Nucléaire de Lyon, CNRS-IN2P3.
[3] Institut Lumière Matière, Université Lyon 1.

E-mail: x.artru@ipnl.in2p3.fr

Abstract. Coherent light production in an optical fiber by a charged particle (named PIGL, for *particle-induced guided light*) is reviewed. From the microscopic point of view, light is emitted by transient electric dipoles induced in the fiber medium by the Coulomb field of the particle. The phenomenon can also considered as the capture of virtual photons of the particle field by the fiber. Two types of captures are distinguished. Type-I takes place in a uniform part of the fiber; then the photon keeps its longitudinal momentum p_z. Type-II takes place near an end or in a non-uniform part of the fiber; then p_z is not conserved. Type-I PIGL is not affected by background lights external to the fiber. At grazing incidence it becomes nearly monochromatic. Its circular polarization depends on the angular momentum of the particle about the fiber and on the relative velocity between the particle and the guided wave. A general formula for the yield of Type-II radiation, based on the reciprocity theorem, is proposed. This radiation can be assisted by metallic objects stuck to the fiber, via plasmon excitation. A periodic structure leads to a *guided Smith-Purcell* radiation. Applications of PIGL in beam diagnostics are considered.

In memory of Karo Asatour Ispirian

1. Introduction

The field of a charged particle passing *through* or *near* an optical fiber induces a transient electric dipole moments of the atoms (see figure 1). Then these dipoles emit radiation coherently. Part of this radiation is channeled by the fiber [1, 2, 3, 4] and we call it *particle-induced guided light* (PIGL). It must not be confused with the incoherent radiation produced in scintillating fibers used as particle detectors. When the fiber radius is much larger than the wavelength, a description in terms of transition- or Cherenkov radiation is appropriate. This is the case for DIRC particle detectors [5, 6, 7]. Here we consider a bare fiber of radius a comparable to the wavelengths, therefore carrying one or a few number of modes. The number of produced photons per particle is too small for individual particle detection, but may be large enough for beam diagnostics. The fiber should have little effect on the beam emittance.

PIGL can also be considered as made of virtual photons from the particle field captured by the fiber. Two types of capture are distinguished.
- Type I : The particle passes *near* or *through* a uniform part of the fiber, far from an end. Then the capture conserves the longitudinal momentum of the photon, p_z.
- Type II : The particle passes near or through an end of the fiber or an added structure (e.g., an indentation or a metallic object touching or close to the fiber). Then p_z is not conserved.

A first investigation of PIGL has been undertaken at Tomsk Polytechnic University [8]. The "fiber" was a dielectric rod of radius $a = 5$ mm and the wavelength domain was 3 - 30 mm. These lengths are about 10^3 times larger than in the optical domain, but the number of PIGL photons is invariant under the rescaling $a \to c\,a$, $\lambda \to c\,\lambda$. In the mm range a very large number of photons is needed to build a detectable signal. This was achieved using the coherent effect of all the electrons in mm size bunches. The set-up configuration shown in [8] is for type-II PIGL.

2. Spectrum of type-I PIGL

We consider a fiber of radius a and uniform index $n = \sqrt{\varepsilon}$ and denote by $\{\mathcal{M}, \omega\}$ the propagation modes. ω is the photon energy[1] and $\mathcal{M} = \{M, n_r, \tau, \sigma\}$ gathers the discrete variables: $M = L_z + S_z$ is the total angular momentum of the photon about the fiber axis $\hat{\mathbf{z}}$; n_r is the radial quantum number; $\sigma = \mathrm{sign}(p)$ indicates the direction of propagation, p being the longitudinal momentum of the photon. τ indicates the mode type: τ=EH for "transverse electric" $[E_z(a) < H_z(a)]$, τ=HE for "transverse magnetic" $[E_z(a) > H_z(a)]$. p and ω are linked by a dispersion relation:

$$\omega = \omega_{\mathcal{M}}(p) \;\leftrightarrow\; p = p_{\mathcal{M}}(\omega)\,. \tag{1}$$

The real electric field of the mode is[2] $\mathbf{E}_{\rm real} = 2\,\mathrm{Re}\{\vec{\mathcal{E}}_{\{\mathcal{M},\omega\}}(\mathbf{X}, t)\, e^{i\eta}\}$, where

$$\vec{\mathcal{E}}_{\{\mathcal{M},\omega\}}(\mathbf{X}, t) = \mathbf{E}_{\{\mathcal{M},\omega\}}(\mathbf{r})\, \exp(ipz - i\omega t) \tag{2}$$

(more precisely $\vec{\mathcal{A}} = -i\vec{\mathcal{E}}/\omega$) is the "photon wave function" and η is a *classical* phase determining the nodes of $\mathbf{E}_{\rm real}$. The transverse coordinate $\mathbf{r} = (x, y)$ is measured from the fiber axis. The dispersion relation and the analytic expressions of the proper fields in a uniform fiber can be found in textbooks [9, 10] or in [1, 3]. Figure 1 shows the phase velocity $v_{\rm ph}(\omega) = \omega/p$ and the group velocity $v_{\rm g}(\omega) = d\omega/dp$ of the lowest mode HE_{11} ($|M|$=1, n_r=1) for n=1.41 (fused silica). The photon spectrum produced in mode $\mathcal{M}$ by an electron of trajectory $\mathbf{X}(t)$ is given by

$$\frac{\omega\, d\mathcal{N}_{\mathcal{M}}}{d\omega} = \frac{1}{2\pi |P_{\mathcal{M}}(\omega)|} \left| e \int_{\rm traj.} d\mathbf{X}(t) \cdot \vec{\mathcal{E}}^{\,*}_{\{\mathcal{M},\omega\}}(\mathbf{X}, t) \right|^2, \tag{3}$$

where $P_{\mathcal{M}}(\omega)$ is the energy flow of the real field:

$$P_{\mathcal{M}}(\omega) = 2 \int d^2\mathbf{r}\; \mathrm{Re}\left\{ \mathbf{E}^*_{\{\mathcal{M},\omega\}}(\mathbf{r}) \times \mathbf{B}_{\{\mathcal{M},\omega\}}(\mathbf{r}) \right\}_z . \tag{4}$$

[1] We use relativistic quantum units units: $\hbar = c = \varepsilon_0 = \mu_0 = 1$. $\lambda\!\!\!^{-} \equiv 1/\omega$. The Gauss law is written $\nabla \cdot \mathbf{E} = \rho$, not $4\pi\rho$. $e^2/(4\pi) = \alpha \simeq 1/137$.

[2] the factor 2 is a question of convention

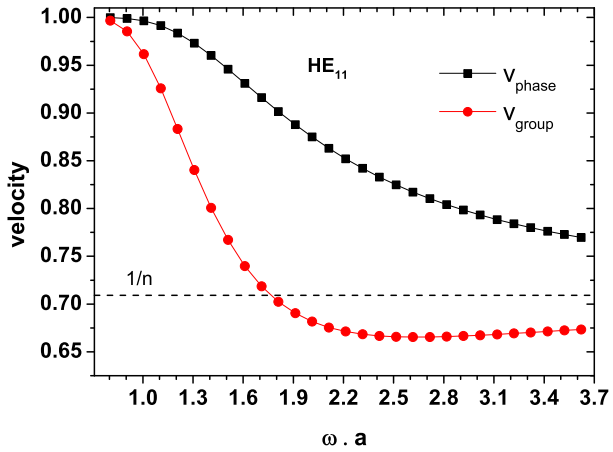

Figure 1. Phase velocity (squares) and group velocity (balls) of the mode HE_{11} as a function of ωa.

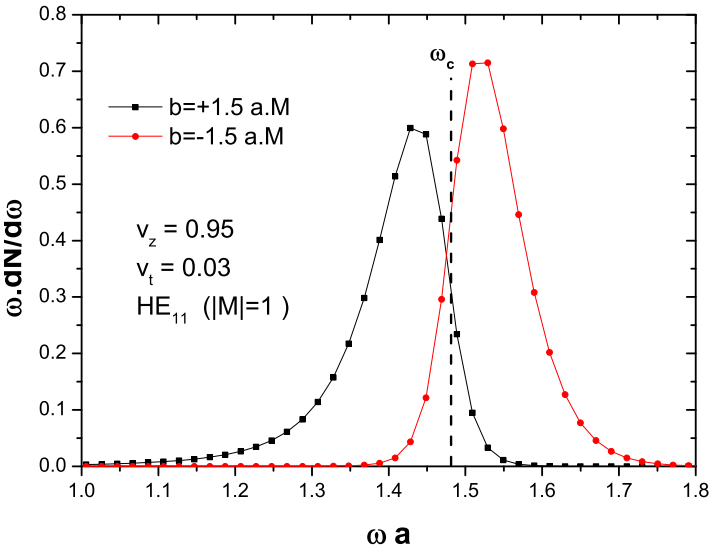

Figure 2. Photon spectra in the HE_{11}, $M{=}\pm1$ modes, for a particle not touching the fiber: $|b| = 1.5\,a$. Squares: bM positive; balls: bM negative. The vertical line is at ω_C defined by Eq.(6). The fiber index is n=1.41.

Some spectra for the HE_{11} mod are presented in Refs.[1, 3] (with an error by a factor 2 in [1]). Figure 2 shows a HE_{11} spectrum for the "passing near" case ($b > a$) and the two helicities. The geometrical parameters are defined in figure 3.

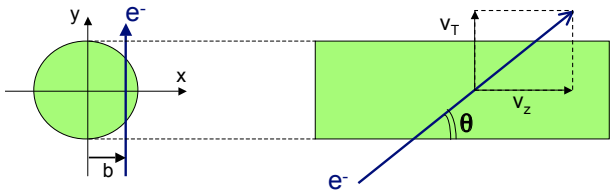

Figure 3. Geometrical parameters of the trajectory. Left side: front view; right side: side view.

Angular drag. In figure 2 one can observe a correlation between the angular momentum of the photon, M, and that of the electron, $J_e = \gamma m_e\,[\mathbf{b}\times\mathbf{v}]\cdot\hat{\mathbf{z}}$:

$$\langle M\rangle J_e \begin{cases} > 0 \text{ if } v_{ph} > v_z \quad (\omega < \omega_C), \\ < 0 \text{ if } v_{ph} < v_z \quad (\omega > \omega_C), \end{cases} \tag{5}$$

where ω_C is the frequency such that the electron "surfes" on the wave :

$$v_{ph}(\mathcal{M}, \omega_C) = v_z(particle)\,. \tag{6}$$

Strictly speeking, inequality (5) is obtained for $\mathbf{v}_T \ll v_z$ [4]. This "angular drag" effect can tell on which side of the fiber a microbeam is passing. An analogous - but opposite - correlation exists in helical undulator radiation, where $\langle M\rangle J_e$ is positive if $v_z(\text{photon}) > v_z(\text{electron})$, i.e., $\theta < 1/\gamma$, negative in the opposite case.

The small angle limit. If the crossing angle θ is small, the radiation in each mode becomes nearly monochromatic about a "Cherenkov peak" $\omega_C(v_z)$ given by (6). The number of photons under the peak is

$$\mathcal{N}_{\mathcal{M}} \simeq \frac{4\pi\alpha}{\omega_C\, P_{\mathcal{M}}(\omega_C)}\; |1/v_g(\omega_C) - 1/v_z|^{-1} \int_{\text{traj.}} dz(t)\; \left|\hat{\mathbf{z}}\cdot\mathbf{E}_{\{\mathcal{M},\omega_C\}}(\mathbf{r}(t))\right|^2 . \tag{7}$$

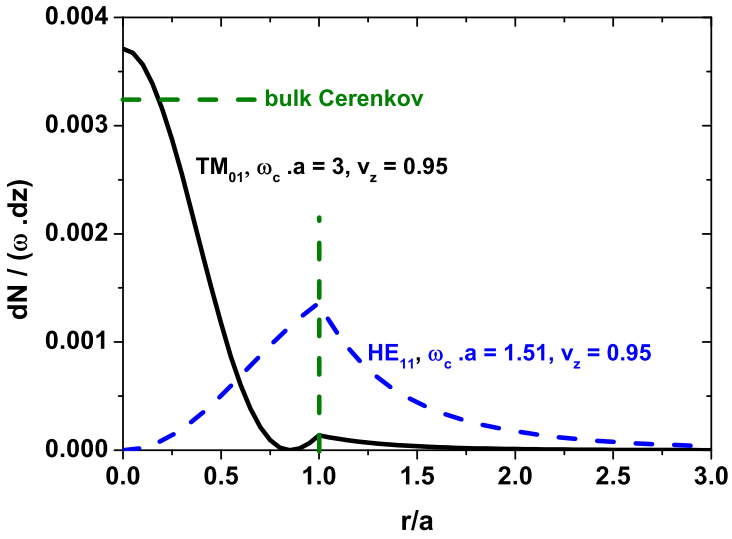

Figure 4. Rate of emitted photon along an electron trajectory at small angle with the fiber, as a function of r. The parameters are v_z=0.95 and $n_{\rm fiber}$=1.41. Peak frequencies: $\omega_{\rm C}$=1.51 a^{-1} for the $\rm HE_{11}$ mode, $\omega_{\rm C}$=3 a^{-1} for the $\rm TM_{01}$ ($\equiv$ $\rm EH_{01}$) mode. The line "bulk Cherenkov" is the spectrum of Cherenkov photon $d\mathcal{N}/d\omega/dz = \alpha\left[1-(nv)^{-2}\right]$ in infinite medium.

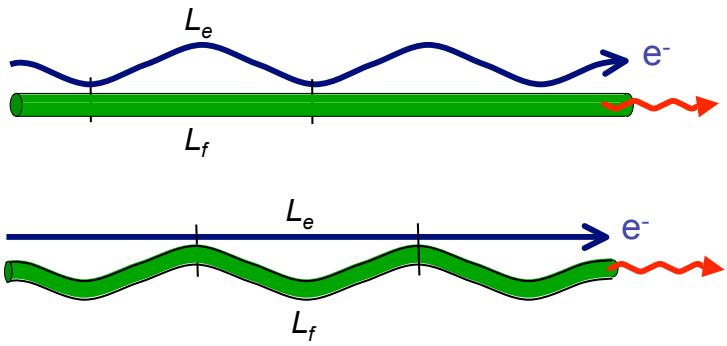

Figure 5. Two types of "fiber undulator".

This formula also applies when the fiber and/or the electron trajectory are weakly curved and at small angle, (x, y, z) being curvilinear coordinates following the fiber axis. Eq.(7) tells that the photon number increases linearly with the time spent by the particle in the region where the longitudinal field of the mode is important. Figure 4 plots $d\mathcal{N}_{\mathcal{M}}/(\omega_{\rm C}\, dz)$ from Eq.(7) as a function of r for the two lowest modes $\rm HE_{11}$ and $\rm TM_{01} \equiv EH_{01}$, at $v_{\rm ph} = v_z$=0.95. This quantity is the number of emitted photons per length $\lambda\!\!\!^{-} \equiv \omega_{\rm C}^{-1}$ of trajectory. $\mathcal{N}_{\mathcal{M}}$ behaves like $1/\theta$ and may exceed unity in spite of the $\alpha = 1/137$ factor. A rough estimation of the peak width is

$$\Delta\omega \sim |v_z/v_{\rm g}(\omega_{\rm C}) - 1|^{-1}\; v_{\rm T}/\max(a, |b|). \tag{8}$$

The exact peak position depends on the sign of $MJ_{\rm e}$, as shown in figure 2. The shift relative to $\omega_{\rm C}$ is comparable to $\Delta\omega$. Strict monochromaticity is obtained when the trajectory is parallel to the fiber. This kind of Cherenkov effect was studied in Refs. [11, 12].

Fiber undulator. If the fiber and/or the particle trajectory are undulated as in figure 5, the peak at $\omega \simeq \omega_{\rm C}$ is split in subpeaks such that

$$\Phi = \omega\; (L_{\rm f}/v_{\rm ph} - L_{\rm e}/v) = 2\pi \times \text{integer}\,, \tag{9}$$

$L_{\rm f}$ and $L_{\rm e}$ being the fiber length and particle path in one period. For a helical undulation a *Berry phase* [13] should be added to the third member of Eq.(9), but it is small for small bending angle.

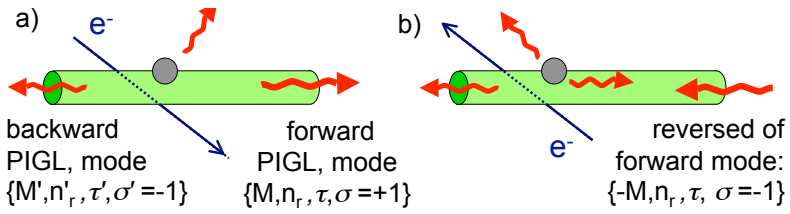

Figure 6. a) waves produced in a type-II PIGL experiment (here using a metallic ball). b) waves in the "inverse PIGL" process for the reciprocity theorem leading to Eq. (10).

3. Type-II PIGL

Figures 6a and 7 present different schemes of type-II photon capture. The PIGL yield may be obtained with a generalization of Eq.(3),

$$\frac{\omega\, d\mathcal{N}_{\mathcal{M}}}{d\omega} = \frac{1}{2\pi|P_{\mathcal{M}}(\omega)|}\left| e\int_{\text{traj.}} d\mathbf{X}(-t)\cdot\vec{\mathcal{E}}_{\{\,\text{rev}\mathcal{M},\omega\},\,\text{in}}\big(\mathbf{X}(-t),t\big)\right|^2, \tag{10}$$

suggested by the reciprocity theorem (or time reversal symmetry), like Eq.(2.33) of [14]. $\mathbf{X}(-t)$ is the time-reversed electron trajectory, $\text{rev}\mathcal{M} = \{-M, n_r, \tau, -\sigma\}$ is the time-reversed mode and "in" refers to the *scattering* wave, solution of the macroscopic Maxwell equations *without the electron*, coming via the fiber *from* the detector direction. This wave contains a reflected part, a transmitted part and an outgoing unguided part indicated by the arrows in figure 6b.

For the schemes of Figs. 6a) and 7a,b,c) the Equivalent Photon method [15, 16] offers an alternative, more direct but less rigourous approach [3, 4]. The photon capture in scheme 7a) is more "adiabatic" than in scheme 7b), hence more efficient. Besides, its angular acceptance is narrower, therefore the background from ambient light is reduced. In schemes 6a), and 7c,d) the particle field excites first a plasmon resonance [17, 18] in the ball(s); then the plasmon

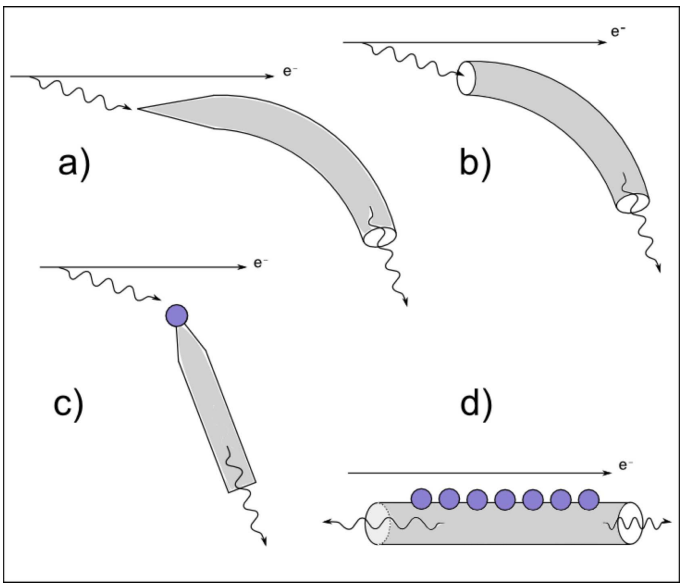

Figure 7. Different schemes of type-II PIGL: a) conical end; b) sharp-cut end; c) metallic ball at one end; d) regularly spaced metallic balls (figure taken from Ref.[3]).

is evacuated with a probability $\mathcal{P}_{\rm f}$ as a photon in the fiber. It yields a quasi-monochromatic spectrum peaked at $\omega_{\rm plasmon} \simeq (4\pi\alpha\, n_e/3m_e)^{1/2}$ which is in the ultraviolet domain.

Guided Smith-Purcell light. In the scheme 7d) the interferences between balls produce peaks at ω such that

$$\Phi \equiv (1/v - 1/v_{\rm ph})\,\omega l = 2\pi \times \text{integer}\,, \tag{11}$$

l being the ball spacing and $\text{sign}(v_{\rm ph}) = +1$ and -1 for forward and backward PIGL respectively. The forward one has the highest frequency. To optimize the photon yield one must choose l such that an interference peak coincides with $\omega_{\rm plasmon}$. In the "kinematical" approach,

$$(d\mathcal{N}_{\mathcal{M}}/d\omega)_{N\text{ balls}} = (d\mathcal{N}_{\mathcal{M}}/d\omega)_{1\text{ ball}} \times \left[\sin^2(N\Phi/2)/\sin^2(\Phi/2)\right]. \tag{12}$$

Re-scattering and *shadowing* [19] by the balls should be taken into account using a "dynamical" theory like in [20]. This type of PIGL, which we call *Guided Smith-Purcell* radiation (GSP), is in competition with the external Smith-Purcell radiation (SP) from the balls, where $1/v_{\rm ph}$ in (11) is replaced by $\cos\theta_{\rm photon}$. If $(1/v + 1/|v_{\rm ph}|)\,\omega l = 2\pi/l$, only backward GSP and no ordinary SP is be emitted, since $|v_{\rm ph}| < 1$. This "exclusivity" reinforces the intensity of backward GSP.

4. Application to beam diagnostics

- Type-I PIGL at large crossing angle can be used for a transverse tomography of the beam with a resolution $\sim 2a$. No background is caused by real photons coming from upstream sources, e.g., synchrotron radiation from upstream bending magnets or transition radiation from an accelerator exit window. Due to p_z conservation, real photons are not captured but only *scattered* by the fiber. This is an advantage over Optical Transition Radiation and Optical Diffraction Radiation. For the same reason the resolution power of type-I PIGL is not affected by the large transverse tail ($\sim \gamma\lambda$) of the virtual photon cloud. Indeed, the virtual photons of this tail are "almost real".

- In microbeam diagnostics the "angular drag" of the circular polarization could tell on which side of the fiber the microbeam is passing.

- In a "fiber undulator" or in Guided Smith-Purcell effect, the width of the interference peaks and the peak/background ratio are sensitive respectively to the velocity and angular spreads of the beam.

- Type-II PIGL at a fiber end can provide directly a 2-dimensional transverse scan of the beam density. It can be assisted by a metallic ball of the type presented in [21, 22] or a SNOM probe. However, like OTR and ODR, it receives the background from upstream radiation sources and is sensitive to the transverse tail of the virtual photon cloud.

- PIGL of type I or II may be used to measure the time profile of the electron bunch. Note that in figure 1 the *group velocity* is almost constant for $\omega \geq 2/a$. Therefore in this frequency domain the signal shape is approximately conserved during the propagation to the detector.

5. Conclusion

We have reviewed the basic mechanism and some important aspects of light generation in monomode or few-mode optical fibers by charged particles (PIGL) : Cherenkov peak for grazing incidence, angular drag, absence of background in type-I, interference peaks for periodic structures or deformations, possibility of using a plasmon resonance. For the photon yield we have given a generalization of the type-I PIGL formula to the type-II case.

Whether or not PIGL can be successfully applied to beam diagnostics is too early to predict. Theoretical and experimental works must be pursued, in particular on the possibility to get a large enough signal, on the heat deposit in the fiber and on the radiation hardness. At least we

can say that the narrowness of monomode fibers without cladding allows a minimal perturbation of the beam and the flexibility of fibers is certainly a great advantage over traditional optical systems.

If the fiber is bent to a radius below $R_{\rm cr} \sim \lambda\ (1-v_{\rm ph}^2)^{-3/2}$ light escapes from it by a tunneling process. The bending loss was investigated in [8]. In Ref. [23] a parallel is made between this effect and synchrotron radiation.

References

[1] Artru X and Ray C 2007, Photon production by charged particles in narrow optical fibers, *Proc. SPIE* **6634** ed Dabagov S B
[2] X. Artru and C. Ray 2008, Interference and shadow effects in the production of light by charged particles in optical fibers, *Nucl. Instr. Methods in Phys. Research* **266** 3725
[3] Artru X and Ray C 2012, Radiation Induced by Charged Particles in Optical Fibers, in *Selected Topics on Optical Fiber Technology* (InTech Open Access Company) ed Yasin M et al
[4] Artru X and Ray C 2013, Light induced by charged particles in optical fibers, *Nucl. Instr. Methods in Phys. Research* B **309** 162
[5] Coyle P et al 1994, *Nucl. Instr. Methods in Phys. Research* A **343** 292
[6] Contin A, De Salvo R, Gorodetzky P, Helleboid J M, Johnson K F, Juillot P, Lazic D and Lundin M 1994, *Nucl. Instr. Methods in Phys. Research* A **367** 271
[7] Janata E 2002, *Nucl. Instr. Methods in Phys. Research* A **493** 1
[8] Naumenko G, Potylitsyn A, Bleko V and Soboleva V 2015, Coherent radiation of relativistic electrons in dielectric fibers, *Nucl. Instr. Methods in Phys. Research* B **335** 125-128
[9] Okoshi T 1982, *Optical Fibers*, Academic Press
[10] Pocholle J P 1985, *L'Optique Guidée Monomode et ses Applications*, ed MASSON
[11] Bogdankevich L S and Bolotovskii B M 1957, *J. Exp. Theoret. Phys.* **32**, 1421 [*Sov. Phys. JETP* **5**, 1157]
[12] Zhevago N K and Glebov V I 1993, *Nucl. Instr. Methods* A **331** 592; 1997 *Zh. Exp. Teor. Fiz.* **111** 466
[13] Tomita A and Chiao R 1986, *Phys. Rev. Lett.* **57** 937
[14] Rullhusen P, Artru X and Dhez P 1998, *Novel Radiation Sources Using Relativistic Electrons*, World Scientific
[15] Jackson JD 1962, *Classical Electrodynamics*, John Wiley & Sons, Inc.
[16] Panofsky W K H and Phillips M 1962, *Classical Electricity and Magnetism*, Addison-Wesley, Inc.
[17] Zhevago N K 1991, *Europhys. Lett.* **15** 277
[18] Yamamoto N, Araya K and García de Abajo F J 2001, *Phys. Rev.* B **64** 205419
[19] Naumenko G, Artru X, Potylitsyn A, Popov Y, Sukhikh L and Shevelev M 2010, *J. Phys.: Conf. Series* **236** 012004
[20] García de Abajo F J 1999, *Phys. Rev. Lett.* **82** 2776; García de Abajo F J 2000, *Phys. Rev.* E **61** 5743
[21] Kalkbrenner T, Ramstein M, Mlynek J and Sandoghdar V 2001, *J. Microsc.* **202** 72
[22] Anger P, Bharadwaj P and Novotny L 2006, *Phys. Rev. Lett.* **96** 113002
[23] Artru X and Ray C 2015, Common characteristics of synchrotron radiation and light leaking from a bent optical fiber (these proceedings)